Published in final edited form as:
J Nucl Cardiol. 2010 June ; 17(3): 498–513. doi:10.1007/s12350-010-9223-5.

Assessment of myocardial perfusion and function with PET and PET/CT

Mouaz H. Al-Mallah, MD, MSc, FACC[c], **Arkadiusz Sitek, PhD**[a], **Stephen C. Moore, PhD**[a], **Marcelo Di Carli, MD**[a,b], and **Sharmila Dorbala, MBBS, FACC**[a]

[a]Division of Nuclear Medicine and Molecular Imaging, Department of Radiology, Brigham and Women's Hospital, Boston, MA

[b]Noninvasive Cardiovascular Imaging Program, Departments of Medicine (Cardiology) and Radiology, Brigham and Women's Hospital, Boston, MA

[c]Cardiology, Henry Ford Hospital, Detroit, MI.

INTRODUCTION

Over the past decade, there has been a growing interest in cardiac imaging with Positron Emission Tomography (PET). However, PET has been used for more than 35 years as a powerful tool to study cardiac physiology. PET started as an investigative tool used at select academic medical centers equipped with cyclotrons, to probe physiologic processes such as myocardial perfusion, metabolism, neuronal innervation, and receptor function. At the outset, myocardial perfusion imaging (MPI) with PET was primarily used in research applications, or as an adjunct to ^{18}F-fluoro deoxy glucose (FDG) imaging for viability assessment, or to guide clinical management in high-risk patients. Over the past 7-8 years, we have witnessed a paradigm shift in the use of MPI with PET. It is now being increasingly used for routine clinical evaluation of patients with known or suspected coronary artery disease (CAD). Also, it is being used not only at large academic institutions, but also at community hospitals and large private practice groups. There are several factors contributing to this shift in the use of PET MPI, including the exponential growth and availability of combined PET + computed tomography (CT) systems which were driven primarily by oncology applications, FDA approval of an easily available generator produced radiotracer, ^{82}Rubidium (Rb), changes in reimbursement, and the increasing clinical evidence supporting the value of PET/CT MPI.

There are several excellent review articles that detail the clinical applications, PET radiotracers,[1] quantitative PET,[2] viability assessment,[3] and utility of hybrid PET MPI applications.[3-6] The focus of this article is to discuss the evolution of PET MPI over the course of the years to highlight some of the major achievements in PET that have culminated in the present day applications of PET MPI.

Reprint requests: Sharmila Dorbala, MBBS, FACC, Division of Nuclear Medicine and Molecular Imaging, Department of Radiology, Brigham and Women's Hospital, Cardiovascular Faculty Offices, Shapiro 5, Room 128, 70 Francis Street, Boston, MA 02115; sdorbala@partners.org..

None of the authors report any conflict of interest.

THE EVOLUTION OF PET AND PET/CT MPI

Technical Developments

Scanners—The initial concept of tomographic emission imaging was introduced by Kuhl and Edwards in the late 1950's and the early 1960's. By the mid-1960's these investigators had also developed an early tomographic device using monoenergetic radionuclides as sources of gamma photons. Soon, thereafter prototype PET devices were developed at the University of Pennsylvania, Washington University (Michael Ter-Pogossian and Michael Phelps), and Massachusetts General Hospital (Brownell and Sweet).7-10 The development of devices continued and PET scanning was introduced to the medical community in the 1970's,11 as a novel technique to study pathophysiological processes. The scanners evolved in the 1980's to more commercial models, with improved image resolution, resulting in the clinical use of cardiac PET. The discovery of the scintillators, bismuth germinate (BGO) (late 1960's to 70's), 12 and subsequently lutetium oxyorthosilicate (LSO) (1990's) led to further improvements in original image quality. The next major breakthrough in technology was the concept of PET/CT (in the early 1990's). A prototype PET/CT scanner was developed (1998) and commercial scanners became available in 2000 (Nutt, Beyer and Townsend). These systems were based on a single-slice CT scanner and enabled faster imaging with greater anatomic information with a single slice CT. This was followed soon thereafter by hybrid devices with enhanced multi-detector computed tomography (MDCT) scanners capable of calcium scoring and CT coronary angiography. Finally, the enormous growth in cardiac PET has fueled the development of a dedicated small foot print PET scanner (Positron corporation, attrius PET scanner) utilizing with radionuclide-based attenuation correction specifically for cardiac applications. Also, although proposed several decades ago,13،14 only recently have some of the PET systems incorporated annihilation-photon time-of-flight (TOF) information during image acquisition; the value of TOF imaging for MPI is unclear at this time.

Simultaneously, several software enhancements have become available. Software was developed for detecting and correcting for misregistration of the transmission and emission images.15 Motion frozen imaging, a concept introduced by Slomka et al16 for SPECT is currently being adapted to PET imaging. Also, novel resolution recovery techniques to improve contrast and contrast noise ratio are under development.[17] Finally, software for quantitative PET and myocardial blood flow (MBF) assessment is rapidly evolving[18-21] and will soon be commercialized for clinical use.

Radiopharmaceuticals—Positron radiopharmaceuticals have been used since the late 1950's.[22,23] In the 1960's, Ter-Pogossian and Powers measured blood flow in the brain using ^{15}O water.[24] In the mid-1960's, quantitative estimation of coronary blood flow was performed with ^{84}Rb, a positron emitter, using a coincidence counting system.[25,26] With the development of biomedical cyclotrons,[27] ^{15}O water and later ^{13}N-ammonia became available for research use in the mid-1970's. ^{15}O water was initially used by Parker et al[28] in 1978 to quantify regional myocardial blood flow (MBF) and regional fractional extraction of oxygen. While myocardial perfusion can be assessed using ^{15}O water, ^{13}N-ammonia, ^{82}Rb, and the new ^{18}F-BMS compound, currently, ^{82}Rb and ^{13}N-ammonia are the only two FDA approved radiotracers.

The initial studies of ^{13}N-ammonia MPI were reported from Dr. Schelbert's[29] and from Dr. Gould's laboratories. Gould et al. demonstrated in intact dogs, that using ^{13}N-ammonia, 47% diameter coronary stenosis can be detected. ^{13}N-ammonia is a cylotron-produced radiotracer (half-life of 9.96 minutes) that was approved by the FDA for assessment of myocardial perfusion in 2000. ^{13}N-ammonia enters the myocyte (passive diffusion or active transport) and is rapidly metabolized to glutamine ^{13}N and retained in the myocyte or can diffuse back into the blood pool.[30,31] Gated ^{13}N-ammonia imaging can provide accurate assessments of both

regional and global cardiac function.[32] However, the use of this imaging agent is limited to centers with a cyclotron and also it is also not well suited for peak stress gated imaging, due to the 3-4 minutes time interval between radiotracer injection and blood pool clearance.

The initial studies with ^{82}Rb MPI were reported by Gould et al.[33-35] ^{82}Rb is a generator produced radiotracer (half-life 76 seconds) that was approved by the FDA for assessment of myocardial perfusion in 1989. It is the most widely used radiotracer for clinical PET MPI.[1] The main advantages of ^{82}Rb are its availability at sites without a cyclotron, rapid imaging protocols, and the ability to obtain peak stress gated imaging. ^{82}Rb has a relatively long positron range (the distance the positron travels before colliding with an electron to release two 511 keV photons), which contributes to its somewhat worse spatial resolution in comparison to ^{18}F or ^{13}N. Also, due to the reduced first-pass extraction of ^{82}Rb, its myocardial uptake is not linear throughout the flow range, i.e., it is characterized by a plateau of uptake at high flow values, resulting in a potential underestimation of flow at maximal hyperemia.[36]

Imaging protocols—Myocardial perfusion PET began as a research tool for quantitative blood flow assessments using dynamic image acquisition (multi frame imaging). The image frames were summed for relative perfusion assessment. Some of the initial PET studies of function included, assessments of lung water content using ^{15}O-water,37 as well as first pass imaging for computing stroke volume, lung water content (a measure that correlated with restrictive filling pattern on echocardiography), and ejection fraction.[38] Gated PET imaging necessitated a separate acquisition with extra time, radiation burden, and imposed greater demands on the processors for image processing and storage. Also, with PET, gated MPI is not necessary for distinguishing attenuation artifacts from scar (due to accurate attenuation correction). Hence, in order to expedite image acquisition and analysis, PET MPI was performed as a nongated study, and echocardiography or radionuclide angiography were used for the assessment of left ventricular ejection fraction (LVEF) and wall motion, when needed. This led to two issues, firstly, LVEF assessment at a temporally different time from the metabolic assessment and next, anatomic co-registration of the perfusion and metabolic image with the wall motion abnormality was difficult.39 Miller et al,39 described the use of inhaled ^{15}O carbon monoxide labeled red blood cell blood pool imaging (used to delineate the vascular pool to correct the ^{15}O-water myocardial perfusion images), and demonstrated that simultaneous assessment of perfusion and function is feasible with ^{15}O-water MPI.

Presently, simultaneous assessment of perfusion and function has become routine practice. The latest PET scanners and computers are very powerful and allow for list mode imaging, i.e., accrual of a list of coincidence-photon detected events along with a recorded ECG and time synchronization signal. List mode acquisitions have greatly enhanced the utility of PET MPI, allowing a comprehensive simultaneous assessment of perfusion and LVEF, and anatomy (with CT when performed) in a single sequence (Figure 1). The current clinically used image acquisition protocols have been well described in the ASNC PET guidelines.[40] All the current clinical imaging protocols are sequential with stress following the rest MPI, with time in between the tests for myocardial radiotracer activity to be decay or diminish by biological pathways. Simultaneous research protocols are being developed wherein rest/stress imaging is done in a single scan to increase throughput, reduce radiation dose, and improve co-registration of the rest and stress emission images.[41]

Attenuation correction—In contrast to SPECT, PET images are always corrected for attenuation. Conventional dedicated PET scanners use radionuclide transmission imaging, whereas, hybrid scanners use CT transmission imaging for measurement and correction of soft-tissue attenuation. Most hybrid scanners do not offer the option of radionuclide transmission imaging. The most commonly used CT protocol is a non-gated low-dose CT in shallow tidal breathing, although end-expiration, end-inspiration, and slow CT protocols have been tried.

42 The accuracy of low-dose CT (10 mA) appears to be comparable to Ge transmission imaging for attenuation correction.[43] However, inaccurate registration of transmission (radionuclide or CT) and emission images from respiratory or patient motion can lead to artifactual defects in 20-40% of cases.15,44-49 Most commercial PET/CT systems now include software tools providing reasonable correction for transmission-emission misalignments from breathing differences or patient movement between the transmission and emission images. However, patient motion during either the transmission or emission imaging limits image quality and cannot be easily corrected using software.50

Stress protocols—Stress testing with PET MPI has been used since the early 1970's. Exercise stress with treadmill or bicycle, pharmacological stress with adenosine, dipyridamole, dobutamine have all been used. Supine bicycle testing was used with PET MPI,[51] but did not gain popularity due to patient motion. Treadmill exercise testing[52,53] with ^{13}N-ammonia and ^{82}Rb were used since the early 1980's. Exercise stress is somewhat cumbersome with ^{82}Rb due to its short half-life, and breathing motion from immediate post exercise imaging. Also, with ^{13}N-ammonia, close coordination with the cyclotron is necessary making it less appealing for routine clinical use in high volume centers. Lastly, the routine use of exercise stress with PET tracers, and close patient contact may significantly increase the radiation exposure to the staff.[54] Therefore, vasodilator stress, dipyridamole, is the most widely used stressor for PET MPI. Handgrip exercise was initially used in conjunction with dipyridamole.[55-57] Subsequently, this practice was abandoned as studies showed that hand grip was associated with higher coronary vascular resistance and reduced peak stress MBF.[58]

Cold pressor testing with PET MPI has been used for the noninvasive assessment of coronary endothelial function and formed the basis for several seminal investigations. Typical protocols include immersion of the foot/hand in ice-cold water (2°C) for 2 minutes, with injection of radiotracer at 1 minute and continued immersion for an additional 1 minute.[59] Unlike vasodilator stressors, which produce a predominantly endothelium independent coronary vasodilator response, cold pressor testing increases MBF indirectly by sympathetic activation, release of norepinephrine from cardiac sympathetic-nerve terminals, which leads to vasodilation via an endothelium-dependent mechanism mediated by NO.60-62

Adenosine has been used with PET since it became available in the early 1990's. It produces maximal hyperemia and is short-lived, but it necessitates two intravenous lines for use with ^{82}Rb, and is hence cumbersome to use. More recently, Regadenoson, an adenosine A2a receptor agonist has been approved for SPECT MPI.[63] Its main advantages include bolus administration with standardized dosing regardless of body weight (single bolus administration of 0.4 mg from a prefilled syringe) and better tolerability. Regadenoson when used in conjunction with ^{82}Rb PET enables ultra-short imaging protocols with complete stress and rest MPI completed in ~17 minutes (Figure 2). The diagnostic accuracy and flow quantitation of PET MPI with Regadenoson are currently being studied.

Quantification of myocardial blood flow—Myocardial blood flow has been quantified in humans for over 40 years.[2] Initially, measurements were based on thermodilution or Doppler techniques during angiography. Radionuclide assessments of regional blood volume,[22] fractional extraction, and blood flow measurements were reported as early as the 1950's using ^{85}Krypton,[64] ^{84}Rb,[65,66] and ^{42}potassium.[67] Over the next two decades,[28,68] these techniques evolved to the use of labeled microspheres (albumin microspheres labeled with ^{68}Ga[69] and ^{11}C-labeled microspheres70) to measure MBF. These investigations led to further development and validation of techniques to quantify MBF with PET.[71-75]

Currently, ^{13}N-ammonia, ^{15}O water, and ^{82}Rb are used for noninvasive MBF quantitation. These tracers have been validated in animal models using microsphere techniques, and their

reproducibility ascertained.[76-81] The short half-life of these tracers enable repeat measurement of blood flow for research applications. ^{15}O-labeled water is an ideal tracer for flow quantitation as its uptake is linearly related to flow and a single compartment model is used for flow quantitation.[2] A 3-compartment model has been developed for blood flow quantitation with ^{13}N-ammonia,[82] while, a two compartment model is used for ^{82}Rb.[2,83] The advantage of ^{82}Rb is that it is widely available at sites without cyclotrons, enabling widespread clinical applicability of absolute blood flow in large number of patients. However, as described earlier, the lower extraction fraction of ^{82}Rb may limit its value for flow quantitation at high flow rates.

DIAGNOSTIC ACCURACY

The coronary circulation is comprised of the large epicardial vessels and the smaller coronary microvascular or resistance vessels. Some of the early investigations in ischemic heart disease with PET, characterized the metabolic changes in the myocardium induced by ischemia.[84] Subsequent studies focused on evaluation of relative and absolute myocardial perfusion assessments. While absolute PET MPI blood flow assessment is helpful to identify coronary microvascular flow abnormalities from a variety of cardiovascular diseases, relative PET MPI blood flow assessment is useful to diagnose epicardial CAD and more widely used clinically.

Evaluation of Coronary Microvascular Dysfunction

Direct imaging of the coronary microvasculature in humans is presently not feasible due to resolution limits of the existing imaging techniques.[85] Abnormalities in endothelial and coronary microvascular function are among the earliest manifestations of atherosclerotic vascular damage and precede overt atherosclerosis. Coronary microvascular function was conventionally assessed by studying MBF changes detected by thermodilution or intracoronary Doppler flow wires, at rest and during intracoronary provocation testing [adenosine (endothelium-independent flow), acetyl choline, papaverine (endothelium-dependent flow)]. The invasive nature of this evaluation limited the diagnosis to a select group of symptomatic individuals requiring invasive coronary angiography. Absolute PET (vasodilator and cold pressor testing) is a direct and precise technique to study microvascular function that is increasingly being used in lieu of intracoronary provocation testing. With the advent of CT coronary angiography, CT can be used to exclude obstructive epicardial CAD and absolute PET MPI to diagnose coronary microvascular flow abnormalities, allowing for non-invasive evaluation of early microvascular dysfunction.

Absolute PET MPI is a powerful tool to evaluate the integrated effects of risk factors on the health of the microvasculature.[85] The magnitude of microvascular dysfunction is directly related to the individual and combined risk factor burden.[86] Indeed, individuals with diabetes,[60,87] dyslipidemia,[88,89] hypertension,[90] and smoking,[91] manifest abnormalities in coronary micro-vascular function even in the absence of underlying obstructive epicardial CAD.[85] Microvascular dysfunction by PET has been described by Dr. Camici's laboratory in primary and secondary left ventricular hypertrophies, hypertrophic92 and dilated cardiomyopathies, 93 and infiltrative heart diseases.85 Also, Zeiher et al[94] demonstrated that endothelial and microvascular dysfunction (from risk factors, and myocardial diseases) contributes to the pathogenesis of myocardial ischemia and predisposes individuals with mild atherosclerosis to exercise-induced ischemia. For a detailed review of coronary microvascular function, the readers are referred to a comprehensive review on this topic.[85]

Diagnosis of Obstructive CAD

In 1974, Gould et al[95] proposed the use of coronary flow reserve (CFR) as a physiologic measure of coronary artery stenosis severity. Subsequent reports[56] extended this concept to the use of PET imaging to assess the functional significance or coronary artery stenoses.

Relative coronary perfusion reserve decreased linearly with ~50% diameter stenosis or ~70% area stenosis of the coronary arteries (Figure 3). In 1975, ^{81}Rb MPI was used by Berman et al[96] to diagnose myocardial ischemia, using planar imaging with a scintillation camera.

Studies of PET and PET/CT MPI—Several studies have since evaluated the diagnostic accuracy of relative PET MPI in the diagnosis of obstructive CAD (Table 1).[97] It is important to note that most of the available data has been obtained with dedicated PET scanners with radionuclide attenuation correction, and using vasodilator stress rather than exercise stress. The average weighted sensitivity of PET MPI for detecting at least one coronary artery with >50% stenosis is 90%, whereas the average specificity is 89%. The corresponding average positive and negative predictive values for the diagnosis of obstructive CAD are 94% and 73%, respectively, and the overall diagnostic accuracy is 90%. The sensitivity of PET for detecting obstructing CAD appears to be equally high in patients with single and multi-vessel (≥2 vessels) disease (92% and 95%, respectively) as well as in overweight and obese individuals (mean BMI>30 kg · m^{-2}), and in men and women.[98]

Comparative studies of PET vs. SPECT—Several studies have compared the diagnostic accuracy of PET vs. SPECT MPI in separate groups of patients.[55,57,99] Go and colleagues compared ^{82}Rb PET and ^{201}Thallium SPECT in 202 patients and demonstrated a higher sensitivity with PET than with SPECT (93% vs. 76%, respectively), without significant changes in specificity (78% vs. 80%, respectively). On the other hand Stewart et al compared ^{82}Rb PET and ^{201}Thallium SPECT in 81 patients and observed a higher specificity for PET than for SPECT (83% vs. 53%, respectively), without significant differences in sensitivity (86% vs. 84%, respectively). The differences between these two studies are likely to be attributable to patient selection resulting in differences in pre-scan likelihood of CAD. More recently, Bateman et al[103] compared ^{82}Rb PET and ^{99m}Tc Sestamibi SPECT in two matched patient cohorts undergoing clinically indicated pharmacologic-stress perfusion imaging using contemporary technology for both SPECT and PET. Overall diagnostic accuracy was higher for PET than for SPECT (89% vs. 79% with a 70% angiographic threshold). The sensitivity of PET MPI to detect obstructive CAD was similar to SPECT MPI, however, the specificity of MPI to exclude obstructive CAD appears was higher for PET compared to SPECT. To directly compare the diagnostic value of PET compared to SPECT MPI, the same patient cohort should undergo both SPECT and PET MPI, both with attenuation correction, especially in obese patients. But such studies are not available yet.

Evaluation of Diffuse CAD

Apex to base gradient—Gould et al[100] described an apex to base perfusion gradient in subjects with mild diffuse angiographic CAD, using relative ^{13}N-ammonia MPI. This gradient was not seen in volunteers and patients with severe obstructive CAD demonstrated discrete perfusion defects without the apex to base gradient (Figure 4). This apex to base gradient was also demonstrated by quantitative ^{13}N-ammonia MPI.[101] The findings of these studies suggest that the apex to base perfusion gradient may indicate underlying diffuse CAD.

Evaluation of Multi-Vessel CAD

Absolute perfusion—The diagnosis of multi-vessel or left main CAD with balanced flow reduction remains a challenge with relative perfusion imaging. In a recent study, nearly 13% of patients with angiographically significant left main stenosis had normal SPECT imaging.[102] As with SPECT, if relative perfusion imaging is used, typically the coronary territory supplied by the most severe stenosis is uncovered by PET and the extent of disease is underestimated in almost 30-50% of patients with multi-vessel obstructive CAD.[103-105]

PET measurements of MBF (in mL · min^{-1} · g^{-1} of myocardium) may also help overcome the limitations of relative perfusion assessments with PET to uncover the presence of multi-vessel CAD. Myocardial blood flow and coronary vasodilator reserve (the ratio between peak hyperemic and rest MBF) are inversely and nonlinearly related to stenosis severity. Quantitative estimates of MBF by PET allows for a better definition of the extent of obstructive CAD.[72,106] If absolute perfusion assessments are used, more global reductions in flow (i.e., balanced ischemia) could be identified (Figure 5).[105] In a study of 23 patients,[105] Rb-82 net retention was quantified as an estimation of absolute perfusion at rest and with dipyridamole stress by use of dynamic PET MPI. Defect sizes were larger with absolute MPI in patients with 3-vessel disease (Table 2). While most of the experience with quantitative perfusion imaging is with ^{13}N-ammonia, quantitative approaches with ^{82}Rb based on factor least squares cardiac factor analysis. Correction for ambiguous solutions in factor analysis using a penalized least squares objective[107] have been developed and validated.[108] Also, software to quantify absolute MBF is being incorporated into commercial packages and should soon be available for routine clinical use.

Left ventricular function—ECG-gating of MPI allows for the assessment of left ventricular volumes and ejection fraction which have proven diagnostic and prognostic utility.[109] Gated PET imaging provides a unique opportunity to assess LVEF at rest and during *peak stress* (as opposed to *post-stress* with gated SPECT). Recent data suggest that in normal subjects, LVEF increases during peak vasodilator stress.[104,110] In the presence of CAD, however, changes in LVEF (from baseline to peak stress) are inversely related to the magnitude of perfusion abnormalities during stress (reflecting myocardium at risk) (Figure 6A) and the extent of angiographic CAD (Figure 6B). An LVEF reserve (stress minus rest LVEF) of ≥5% has a negative predictive value of 97% to exclude the presence of three-vessel and/or left main CAD.[104]

Finally, CT coronary angiography and calcium scoring are important adjuncts for identifying more extensive disease than is evident on relative PET MPI.

RISK STRATIFICATION

Semi-Quantitative Relative Perfusion

Given its recent adoption in the routine clinical imaging services, studies documenting the prognostic value of PET MPI in predicting patient's outcomes are few, but beginning to emerge (Table 3). Overall, all the studies demonstrated an excellent outcome with normal MPI; increases in the extent and severity of stress perfusion defects translated into proportional increases in predicted mortality. Of note, the patient cohort in the study by Marwick et al[111] was comprised of high risk patients, with 84% of patients having had prior coronary angiography, and reflecting the utilization of PET during the early 1990's. Yoshinaga et al[112] studied a more contemporary cohort of patients, but their study was limited by the smaller patient cohort, and limited number of cardiac events. Subsequent studies[113,114] confirmed the prognostic value of ^{82}Rb PET MPI in larger patient cohorts. The incremental prognostic value of ^{82}Rb MPI over demographic variables, stress variables, and rest LVEF (Figure 7A and B) was also demonstrated.[113]

Left Ventricular Function

Regional wall motion and LVEF obtained using echocardiography or radionuclide angiography have been used in conjunction with PET viability assessment for the past several decades to improve predictive accuracy for identification of myocardial segments that may improve function following revascularization. For instance, Yoshida et al demonstrated that large infarct size and absence of viable myocardium as assessed by ^{82}Rb, as well as low LVEF

determine adverse outcomes in patients with CAD.[115] However, since LVEF was not routinely assessed with PET MPI, unlike SPECT,[109] data about the prognostic value of LVEF in conjunction with MPI are just beginning to emerge. The study by Lertsburapa et al,[114] was the first to demonstrate that the addition of stress LVEF to clinical and perfusion variables significantly enhanced the value of the ^{82}Rb MPI to predict all cause mortality. Also, in the study by Dorbala et al, in 985 patients with peak stress gated data, the annualized rates of cardiac events (2.1% vs. 5.3%, $P<.001$) and all-cause death (4.3% vs. 9.2%, $P<.001$) were higher in patients with an LVEF reserve <0% compared with those with an LVEF reserve 0%. Multivariable risk adjusted analysis demonstrated independent and incremental prognostic value of LVEF reserve compared to clinical variables, rest LVEF, and MPI.

Absolute Perfusion

A few studies have shown that coronary vasodilator reserve assessed by rest and vasodilator PET can assess progression of CAD and stratify risk of future cardiovascular outcomes. Gould et al[116] demonstrated that a modest regression of coronary artery stenoses after risk factor modification is associated with decreased size and severity of perfusion abnormalities on rest-dipyridamole PET. These results suggest that progression or regression of CAD in response to therapy can be followed non-invasively by absolute PET MPI. Also, in 51 subjects with hypertrophic cardiomyopathy followed for 8 years, those with the lowest tertile of ^{13}N ammonia dipyridamole MBF at baseline had significantly worse long-term clinical outcomes. 92 Similarly, the degree of coronary microvascular dysfunction has been shown to be an independent predictor of death and progressive heart failure in patients with dilated cardiomyopathy.93 Lastly, Herzog and colleagues[117] reported that coronary flow reserve (CFR) could add incremental prognostic value to semi quantitative MPI in predicting hard and soft endpoints in a study of 256 patients who underwent ^{13}N-ammonia PET. In patients with normal perfusion, abnormal CFR was independently associated with a higher annual event rate over 3 years compared with normal CFR for cardiac events (1.4% vs. 6.3%; $P<.05$) and cardiac death (0.5% vs. 3.1%; $P<.05$).[118] Although this study was limited by the small event rate, it is the first study to report the prognostic value of absolute PET MPI in patients with known or suspected CAD.

All of the aforementioned studies demonstrated the prognostic value of vasodilator perfusion reserve, a measure of predominantly endothelium independent mechanisms of MBF. The prognostic value of endothelial-dependent flow abnormalities, were studied by Schindler et al[59] using rest and cold pressor stress MPI in 72 subjects without epicardial CAD. This study demonstrated that impaired or decreased MBF response to cold pressor test may stratify risk of future cardiovascular events. However, on multivariable analysis, cardiac events were independently related to hypercholesterolemia, hypertension, smoking, increases in body mass index, but not to impaired MBF response to cold pressor test, suggesting that impaired CFR may be a marker of risk reflecting the effects of atherogenic risk factor burden.

COMBINED PET AND CT APPLICATIONS

A detailed discussion of combined PET and CT applications is beyond the scope of this review. The ability to image myocardial perfusion along with anatomic atherosclerosis (calcium scoring or CT coronary angiogram) is a major advantage of the hybrid PET/CT scanners compared to dedicated PET scanners. While these offer several interesting clinical applications, the costs of combined imaging and radiation burden need to be considered. Also, the challenges of interpreting the non-cardiac ancillary findings on the low-dose CT scan are not trivial. At this time there is no consensus on whether these non-diagnostic CT scans should be routinely reviewed for ancillary findings.

Calcium Score

Recent data suggest that quantification of coronary artery calcium (CAC) score at the time of stress MPI with PET/CT adds incremental prognostic information to MPI.[119] In a consecutive series of 621 patients undergoing stress PET imaging and CAC scoring in the same clinical setting, there was an increase in events (death and myocardial infarction) with increasing levels of CAC score for any given degree of perfusion abnormality. Indeed, the annualized event rate in patients with normal MPI and no CAC was substantially lower than among those with normal MPI and a CAC ≥ 1,000 (Figure 8). The results of this and other studies suggest the utility of the knowledge of anatomic atherosclerosis in conjunction with physiologic data while performing PET MPI.[120] Some investigators propose routine calcium scoring with PET/CT MPI in patients without known CAD, but, the effectiveness of this approach needs to be further evaluated.

CT Coronary Angiography

Advances in cardiac CT have accelerated in the past few years. With the use of multi-detector CT systems, coronary CT angiography has been shown to have high negative predictive value for ruling out CAD. However, cardiac CT is limited by its modest positive predictive value.[121] With the use of CT dose-reducing techniques (step and shoot imaging (prospective triggering), ECG dose modulation, low KVp imaging etc.) hybrid PET and CT angiography imaging could be performed (on the same or separate scanners) with a relatively low radiation exposure.[122,123] Hybrid PET and CT coronary angiography may be useful in identifying more extensive CAD, balanced ischemia, microvascular dysfunction, coronary anomalies, structural abnormalities of the coronary arteries and their functional consequences and at clarifying equivocal findings on either the CTA or the PET MPI. Hybrid imaging may also be useful in defining the vessel responsible for a perfusion defect seen on PET MPI (Figure 9). Further research is underway focusing on identifying the patient population that would benefit from combined anatomical and perfusion imaging.[124] Combined PET/CT imaging offers great potential for molecular imaging applications with targeted radiotracers, with the CT image serving as the anatomic roadmap for localization of the radiotracer uptake.

RADIATION EXPOSURE WITH PET AND PET/CT

Radiation exposure from cardiovascular imaging has become a major public health concern given the increase in the utilization of diagnostic testing. The estimated effective dose estimates for various cardiac PET/CT procedures are listed in the Table 4.[125-127] Multiple steps should be taken to reduce radiation exposure in PET MPI including ensuring the appropriateness of the study, reducing the amount of injected dose, using low-dose CT for attenuation correction, using 3D PET imaging with a smaller dose of radioactivity, and possibly considering stress-only imaging.[128]

FUTURE DIRECTIONS

New Perfusion Agents

It has been a long time since a new myocardial perfusion agent for PET imaging has been introduced. However, studies are ongoing with new novel agents. Recently, Nekolla et al[129] reported on a new ^{18}F-labeled perfusion agent, ^{18}F-BMS-747158-02 (^{18}F-BMS) in a porcine transient ischemia model, with comparisons to myocardial uptake with ^{13}N ammonia and radioactive microspheres. Compared with $^{13}NH_3$, ^{18}F-BMS showed higher activity ratios between myocardium and blood (rest 2.5 vs. 4.1; stress 2.1 vs. 5.8), liver (rest 1.2 vs. 1.8; stress 0.7 vs. 2.0), and lungs (rest 2.5 vs. 4.2; stress 2.9 vs. 6.4). Regional MBF assessed with ^{18}F-BMS PET showed excellent correlation (r = .88). In addition, ^{18}F-BMS showed homogeneously high and stable cardiac uptake and its image quality was rated superior to that

of the ^{13}N ammonia images by blinded observers (Figure 10). In the isolated perfused rat heart, ^{18}F-BMS demonstrated a high first-pass extraction (above 90%). These results are encouraging and are currently being tested in Phase 2 clinical studies. If successful, this new agent holds promise for significantly expanding the clinical use of PET MPI, by providing the option of unit dose PET radiotracers (akin to SPECT tracers).

CONCLUSIONS

We have reviewed the evolution of PET and some of the major developments in myocardial perfusion and function imaging by PET. PET is a robust and mature technique to non-invasively study myocardial perfusion and function. The rapidly accumulating investigative evidence to support the utility of PET MPI, combined with the developments in scanners, software, and novel radiotracers, will lead to greater clinical use of cardiac PET imaging. The availability of absolute perfusion measurements and investigations into targeted molecular imaging will likely further enhance the clinical applications of PET MPI in the future.

Acknowledgments

ResearchGrants: GE Healthcare, Bracco Diagnostics, Siemens and Astellas.

References

1. Beller GA, Bergmann SR. Myocardial perfusion imaging agents: SPECT and PET. J Nucl Cardiol 2004;11:71–86. [PubMed: 14752475]
2. Rimoldi OE, Camici PG. Positron emission tomography for quantitation of myocardial perfusion. J Nucl Cardiol 2004;11:482–90. [PubMed: 15295417]
3. Di Carli MF. Advances in positron emission tomography. J Nucl Cardiol 2004;11:719–32. [PubMed: 15592196]
4. Bengel FM, Higuchi T, Javadi MS, Lautamaki R. Cardiac positron emission tomography. J Am Coll Cardiol 2009;54:1–15. [PubMed: 19555834]
5. Di Carli MF, Dorbala S, Meserve J, El Fakhri G, Sitek A, Moore SC. Clinical myocardial perfusion PET/CT. J Nucl Med 2007;48:783–93. [PubMed: 17475968]
6. Di Carli MF, Hachamovitch R. New technology for noninvasive evaluation of coronary artery disease. Circulation 2007;115:1464–80. [PubMed: 17372188]
7. Brownell GL, Sweet WH. Scanning of positron-emitting isotopes in diagnosis of intracranial and other lesions. Acta Radiol 1956;46:425–34. [PubMed: 13361957]
8. Sweet WH, Brownell GL. Localization of intracranial lesions by scanning with positron-emitting arsenic. J Am Med Assoc 1955;157:1183–8. [PubMed: 14353655]
9. [Accessed 2/1/2010]. at http://interactive.snm.org/index.cfm?PageID=1107&RPID=10
10. http://www.mit.edu/~glb/alb.html
11. Phelps ME, Hoffman EJ, Coleman RE, et al. Tomographic images of blood pool and perfusion in brain and heart. J Nucl Med 1976;17:603–12. [PubMed: 818345]
12. Dahlbom M, Hoffman EJ. An evaluation of a two-dimensional array detector for high resolution PET. IEEE Trans Med Imaging 1988;7:264–72. [PubMed: 18230478]
13. Brownell GL, Burnham CA, Wilensky S, et al. New developments in positron scintigraphy and the application of cyclotron produced positron emitters. Med Radioisotope Scintigr 1969;968(I):46.
14. Ter-Pogossian MM, Mullani NA, Ficke DC, Markham J, Snyder DL. Photon time-of-flight-assisted positron emission tomography. J Comput Assist Tomogr 1981;5:227–39. [PubMed: 6971303]
15. Kennedy JA, Israel O, Frenkel A. Directions and magnitudes of misregistration of CT attenuation-corrected myocardial perfusion studies: Incidence, impact on image quality, and guidance for reregistration. J Nucl Med 2009;50:1471–8. [PubMed: 19690038]
16. Slomka PJ, Nishina H, Berman DS, et al. “Motion-frozen” display and quantification of myocardial perfusion. J Nucl Med 2004;45:1128–34. [PubMed: 15235058]

17. Le Meunier L, Slomka PJ, Dey D, et al. Enhanced definition PET for cardiac imaging. J Nucl Cardiol. 2010 in press.
18. El Fakhri G, Kardan A, Sitek A, et al. Reproducibility and accuracy of quantitative myocardial blood flow assessment with (82)Rb PET: Comparison with (13)N-ammonia PET. J Nucl Med 2009;50:1062–71. [PubMed: 19525467]
19. El Fakhri G, Sitek A, Zimmerman RE, Ouyang J. Generalized five-dimensional dynamic and spectral factor analysis. Med Phys 2006;33:1016–24. [PubMed: 16696478]
20. Nesterov SV, Han C, Maki M, et al. Myocardial perfusion quantitation with 15O-labelled water PET: High reproducibility of the new cardiac analysis software (Carimas). Eur J Nucl Med Mol Imaging 2009;36:1594–602. [PubMed: 19408000]
21. Slomka PJ, Berman DS, Germano G. Applications and software techniques for integrated cardiac multimodality imaging. Expert Rev Cardiovasc Ther 2008;6:27–41. [PubMed: 18095905]
22. Spratt JS Jr, Ter-Pogossian M, Rudman S, Spencer A. The measurement of the pulmonary venous crosscirculation through the conjugated heart of thoracopagous twins with radioactive O15. Surgery 1961;50:941–6. [PubMed: 13915918]
23. Spratt JS Jr, Ter-Pogossian M, Rudman S, Spencer A. Radioactive oxygen-15 in the tracer study of oxygen transport. Surg Forum 1961;12:7–9. [PubMed: 13915917]
24. Ter-Pogossian MM, Eichling JO, Davis DO, Welch MJ, Metzger JM. The determination of regional cerebral blood flow by means of water labeled with radioactive oxygen 15. Radiology 1969;93:31–40. [PubMed: 5801139]
25. Bing RJ, Bennish A, Bluemchen G, Cohen A, Gallagher JP, Zaleski EJ. The determination of coronary flow equivalent with coincidence counting technic. Circulation 1964;29:833–46. [PubMed: 14172092]
26. Cohen A, Gallagher JP, Luebs ED, et al. The quantitative determination of coronary flow with a positron (rubidium-84). Circulation 1965;32:636–49. [PubMed: 4953256]
27. Ter-Pogossian MM, Wagner HN Jr. A new look at the cyclotron for making short-lived isotopes. 1966-classical article. Semin Nucl Med 1998;28:202–12. [PubMed: 9704362]
28. Parker JA, Beller GA, Hoop B, Holman BL, Smith TW. Assessment of regional myocardial blood flow and regional fractional oxygen extraction in dogs, using 15O-water and 15O-hemoglobin. Circ Res 1978;42:511–8. [PubMed: 630668]
29. Schelbert HR, Phelps ME, Hoffman EJ, Huang SC, Selin CE, Kuhl DE. Regional myocardial perfusion assessed with N-13 labeled ammonia and positron emission computerized axial tomography. Am J Cardiol 1979;43:209–18. [PubMed: 760475]
30. Monahan WG, Tilbury RS, Laughlin JS. Uptake of 13 N-labeled ammonia. J Nucl Med 1972;13:274–7. [PubMed: 5011778]
31. Schelbert HR, Phelps ME, Huang SC, et al. N-13 ammonia as an indicator of myocardial blood flow. Circulation 1981;63:1259–72. [PubMed: 7226473]
32. Hickey KT, Sciacca RR, Bokhari S, et al. Assessment of cardiac wall motion and ejection fraction with gated PET using N-13 ammonia. Clin Nucl Med 2004;29:243–8. [PubMed: 15096971]
33. Gould KL, Goldstein RA, Mullani NA, et al. Noninvasive assessment of coronary stenoses by myocardial perfusion imaging during pharmacologic coronary vasodilation. VIII. Clinical feasibility of positron cardiac imaging without a cyclotron using generator-produced rubidium-82. J Am Coll Cardiol 1986;7:775–89. [PubMed: 3485669]
34. Demer LL, Gould KL, Goldstein RA, et al. Assessment of coronary artery disease severity by positron emission tomography. Comparison with quantitative arteriography in 193 patients. Circulation 1989;79:825–35. [PubMed: 2784361]
35. Gould KL, Schelbert HR, Phelps ME, Hoffman EJ. Noninvasive assessment of coronary stenoses with myocardial perfusion imaging during pharmacologic coronary vasodilatation. V. Detection of 47 percent diameter coronary stenosis with intravenous nitrogen-13 ammonia and emission-computed tomography in intact dogs. Am J Cardiol 1979;43:200–8. [PubMed: 760474]
36. Selwyn AP, Allan RM, L'Abbate A, et al. Relation between regional myocardial uptake of rubidium-82 and perfusion: Absolute reduction of cation uptake in ischemia. Am J Cardiol 1982;50:112–21. [PubMed: 6979917]

37. Ahluwalia BD, Brownell GL, Hales CA, Kazemi H. An index of pulmonary edema measured with emission computed tomography. J Comput Assist Tomogr 1981;5:690–4. [PubMed: 6975288]
38. Sorensen J, Andren B, Blomquist G, Stahle E, Langstrom B, Hedenstierna G. The central circulation in congestive heart failure non-invasively evaluated with dynamic positron emission tomography. Clin Physiol Funct Imaging 2006;26:171–7. [PubMed: 16640513]
39. Miller TR, Wallis JW, Landy BR, Gropler RJ, Sabharwal CL. Measurement of global and regional left ventricular function by cardiac PET. J Nucl Med 1994;35:999–1005. [PubMed: 8195887]
40. Dilsizian, V.; Bacharach, SL.; Beanlands, RS.; Bergmann, SR.; Delbeke, D.; Gropler, RJ., et al. PET myocardial perfusion and metabolism clinical imaging. 2008. http://wwwasncorg/imageuploads/ImagingGuidelinesPETJuly2009pdf
41. Rust TC, DiBella EV, McGann CJ, Christian PE, Hoffman JM, Kadrmas DJ. Rapid dual-injection single-scan 13 N-ammonia PET for quantification of rest and stress myocardial blood flows. Phys Med Biol 2006;51:5347–62. [PubMed: 17019043]
42. Bacharach SL. PET/CT attenuation correction: Breathing lessons. J Nucl Med 2007;48:677–9. [PubMed: 17475952]
43. Koepfli P, Hany TF, Wyss CA, et al. CT attenuation correction for myocardial perfusion quantification using a PET/CT hybrid scanner. J Nucl Med 2004;45:537–42. [PubMed: 15073247]
44. Lang N, Dawood M, Buther F, Schober O, Schafers M, Schafers K. Organ movement reduction in PET/CT using dual-gated list-mode acquisition. Z Med Phys 2006;16:93–100. [PubMed: 16696375]
45. Lautamaki R, Brown TL, Merrill J, Bengel FM. CT-based attenuation correction in (82)Rb-myocardial perfusion PET-CT: Incidence of misalignment and effect on regional tracer distribution. Eur J Nucl Med Mol Imaging 2008;35:305–10. [PubMed: 17909791]
46. Le Meunier L, Maass-Moreno R, Carrasquillo JA, Dieckmann W, Bacharach SL. PET/CT imaging: Effect of respiratory motion on apparent myocardial uptake. J Nucl Cardiol 2006;13:821–30. [PubMed: 17174813]
47. McQuaid SJ, Hutton BF. Sources of attenuation-correction artefacts in cardiac PET/CT and SPECT/CT. Eur J Nucl Med Mol Imaging 2008;35:1117–23. [PubMed: 18219483]
48. Gould KL, Pan T, Loghin C, Johnson NP, Guha A, Sdringola S. Frequent diagnostic errors in cardiac PET/CT due to misregistration of CT attenuation and emission PET images: A definitive analysis of causes, consequences, and corrections. J Nucl Med 2007;48:1112–21. [PubMed: 17574974]
49. Loghin C, Sdringola S, Gould KL. Common artifacts in PET myocardial perfusion images due to attenuation-emission mis-registration: Clinical significance, causes, and solutions. J Nucl Med 2004;45:1029–39. [PubMed: 15181138]
50. Naum A, Laaksonen MS, Tuunanen H, et al. Motion detection and correction for dynamic (15)O-water myocardial perfusion PET studies. Eur J Nucl Med Mol Imaging 2005;32:1378–83. [PubMed: 16142471]
51. Krivokapich J, Smith GT, Huang SC, et al. 13 N ammonia myocardial imaging at rest and with exercise in normal volunteers. Quantification of absolute myocardial perfusion with dynamic positron emission tomography. Circulation 1989;80:1328–37. [PubMed: 2805269]
52. Chow BJ, Ananthasubramaniam K, dekemp RA, Dalipaj MM, Beanlands RS, Ruddy TD. Comparison of treadmill exercise versus dipyridamole stress with myocardial perfusion imaging using rubidium-82 positron emission tomography. J Am Coll Cardiol 2005;45:1227–34. [PubMed: 15837254]
53. Chow BJ, Beanlands RS, Lee A, et al. Treadmill exercise produces larger perfusion defects than dipyridamole stress N-13 ammonia positron emission tomography. J Am Coll Cardiol 2006;47:411–6. [PubMed: 16412870]
54. Schleipman AR, Castronovo FP Jr, Di Carli MF, Dorbala S. Occupational radiation dose associated with Rb-82 myocardial perfusion positron emission tomography imaging. J Nucl Cardiol 2006;13:378–84. [PubMed: 16750783]
55. Go RT, Marwick TH, MacIntyre WJ, et al. A prospective comparison of rubidium-82 PET and thallium-201 SPECT myocardial perfusion imaging utilizing a single dipyridamole stress in the diagnosis of coronary artery disease. J Nucl Med 1990;31:1899–905. [PubMed: 2266384]

56. Goldstein RA, Kirkeeide RL, Demer LL, et al. Relation between geometric dimensions of coronary artery stenoses and myocardial perfusion reserve in man. J Clin Invest 1987;79:1473–8. [PubMed: 3494749]
57. Stewart RE, Schwaiger M, Molina E, et al. Comparison of rubidium-82 positron emission tomography and thallium-201 SPECT imaging for detection of coronary artery disease. Am J Cardiol 1991;67:1303–10. [PubMed: 2042560]
58. Czernin J, Auerbach M, Sun KT, Phelps M, Schelbert HR. Effects of modified pharmacologic stress approaches on hyperemic myocardial blood flow. J Nucl Med 1995;36:575–80. [PubMed: 7699444]
59. Schindler TH, Nitzsche EU, Schelbert HR, et al. Positron emission tomography-measured abnormal responses of myocardial blood flow to sympathetic stimulation are associated with the risk of developing cardiovascular events. J Am Coll Cardiol 2005;45:1505–12. [PubMed: 15862426]
60. Prior JO, Quinones MJ, Hernandez-Pampaloni M, et al. Coronary circulatory dysfunction in insulin resistance, impaired glucose tolerance, and type 2 diabetes mellitus. Circulation 2005;111:2291–8. [PubMed: 15851590]
61. Jones CJ, DeFily DV, Patterson JL, Chilian WM. Endothelium-dependent relaxation competes with alpha 1- and alpha 2-adrenergic constriction in the canine epicardial coronary microcirculation. Circulation 1993;87:1264–74. [PubMed: 8384938]
62. Kichuk MR, Seyedi N, Zhang X, et al. Regulation of nitric oxide production in human coronary microvessels and the contribution of local kinin formation. Circulation 1996;94:44–51. [PubMed: 8964116]
63. Al Jaroudi W, Iskandrian AE. Regadenoson: A new myocardial stress agent. J Am Coll Cardiol 2009;54:1123–30. [PubMed: 19761931]
64. Hansen AT, Haxholdt BF, Husfeldt E, et al. Measurement of coronary blood flow and cardiac efficiency in hypothermia by use of radioactive krypton 85. Scand J Clin Lab Invest 1956;8:182–8. [PubMed: 13390812]
65. Love WD, Burch GE. Differences in the rate of Rb86 uptake by several regions of the myocardium of control dogs and dogs receiving 1-norepinephrine or pitressin. J Clin Invest 1957;36:479–84. [PubMed: 13406062]
66. Cohen A, Zaleski EJ, Luebs ED, Bing RJ. The use of positron emitter in the determination of coronary blood flow in man. J Nucl Med 1965;6:651–66. [PubMed: 4953629]
67. Donato L, Bartolomei G, Giordani R. Evaluation of myocardial blood perfusion in man with radioactive potassium or rubidium and precordial counting. Circulation 1964;29:195–203. [PubMed: 14119384]
68. Cannon PJ, Dell RB, Dwyer EM Jr. Regional myocardial perfusion rates in patient with coronary artery disease. J Clin Invest 1972;51:978–94. [PubMed: 5062613]
69. Wisenberg G, Schelbert HR, Hoffman EJ, et al. In vivo quantitation of regional myocardial blood flow by positron-emission computed tomography. Circulation 1981;63:1248–58. [PubMed: 6971715]
70. Selwyn AP, Shea MJ, Foale R, et al. Regional myocardial and organ blood flow after myocardial infarction: Application of the microsphere principle in man. Circulation 1986;73:433–43. [PubMed: 3485017]
71. Kaufmann PA, Gnecchi-Ruscone T, Yap JT, Rimoldi O, Camici PG. Assessment of the reproducibility of baseline and hyperemic myocardial blood flow measurements with 15O-labeled water and PET. J Nucl Med 1999;40:1848–56. [PubMed: 10565780]
72. Muzik O, Beanlands RS, Hutchins GD, Mangner TJ, Nguyen N, Schwaiger M. Validation of nitrogen-13-ammonia tracer kinetic model for quantification of myocardial blood flow using PET. J Nucl Med 1993;34:83–91. [PubMed: 8418276]
73. Sawada S, Muzik O, Beanlands RS, Wolfe E, Hutchins GD, Schwaiger M. Interobserver and interstudy variability of myocardial blood flow and flow-reserve measurements with nitrogen 13 ammonia-labeled positron emission tomography. J Nucl Cardiol 1995;2:413–22. [PubMed: 9420821]
74. Schelbert HR, Phelps ME, Hoffman E, Huang SC, Kuhl DE. Regional myocardial blood flow, metabolism and function assessed noninvasively with positron emission tomography. Am J Cardiol 1980;46:1269–77. [PubMed: 7006368]

75. Huesman RH, Klein GJ, Reutter BW, Coxson PG, Botvinick EH, Budinger TF. Strategies for extraction of quantitative data from volumetric dynamic cardiac positron emission tomography data. Cardiology 1997;88:54–61. [PubMed: 8960627]
76. Herrero P, Kim J, Sharp TL, et al. Assessment of myocardial blood flow using 15O-water and 1-11C-acetate in rats with small-animal PET. J Nucl Med 2006;47:477–85. [PubMed: 16513617]
77. Utley J, Carlson EL, Hoffman JI, Martinez HM, Buckberg GD. Total and regional myocardial blood flow measurements with 25 micron, 15 micron, 9 micron, and filtered 1-10 micron diameter microspheres and antipyrine in dogs and sheep. Circ Res 1974;34:391–405. [PubMed: 4818762]
78. Lautamaki R, George RT, Kitagawa K, et al. Rubidium-82 PET-CT for quantitative assessment of myocardial blood flow: Validation in a canine model of coronary artery stenosis. Eur J Nucl Med Mol Imaging 2009;36:576–86. [PubMed: 18985343]
79. Knuuti J, Kajander S, Maki M, Ukkonen H. Quantification of myocardial blood flow will reform the detection of CAD. J Nucl Cardiol 2009;16:497–506. [PubMed: 19495903]
80. Lekx KS, deKemp RA, Beanlands RS. 3D versus 2D dynamic 82Rb myocardial blood flow imaging in a canine model of stunned and infarcted myocardium. Nucl Med Commun 2010;31:75–81. [PubMed: 19838136]
81. Lekx KS, deKemp RA, Beanlands RS, et al. Quantification of regional myocardial blood flow in a canine model of stunned and infarcted myocardium: Comparison of rubidium-82 positron emission tomography with microspheres. Nucl Med Commun 2010;31:67–74. [PubMed: 19823095]
82. Hutchins GD, Schwaiger M, Rosenspire KC, Krivokapich J, Schelbert H, Kuhl DE. Noninvasive quantification of regional blood flow in the human heart using N-13 ammonia and dynamic positron emission tomographic imaging. J Am Coll Cardiol 1990;15:1032–42. [PubMed: 2312957]
83. Herrero P, Markham J, Shelton ME, Bergmann SR. Implementation and evaluation of a two-compartment model for quantification of myocardial perfusion with rubidium-82 and positron emission tomography. Circ Res 1992;70:496–507. [PubMed: 1537087]
84. Weiss ES, Hoffman EJ, Phelps ME, et al. External detection and visualization of myocardial ischemia with 11C-substrates in vitro and in vivo. Circ Res 1976;39:24–32. [PubMed: 776436]
85. Camici PG, Crea F. Coronary microvascular dysfunction. N Engl J Med 2007;356:830–40. [PubMed: 17314342]
86. Dorbala S, Hassan A, Heinonen T, Schelbert HR, Di Carli MF. Coronary vasodilator reserve and Framingham risk scores in subjects at risk for coronary artery disease. J Nucl Cardiol 2006;13:761–7. [PubMed: 17174807]
87. Di Carli MF, Bianco-Batlles D, Landa ME, et al. Effects of autonomic neuropathy on coronary blood flow in patients with diabetes mellitus. Circulation 1999;100:813–9. [PubMed: 10458716]
88. Pitkanen OP, Raitakari OT, Niinikoski H, et al. Coronary flow reserve is impaired in young men with familial hypercholesterolemia. J Am Coll Cardiol 1996;28:1705–11. [PubMed: 8962555]
89. Dayanikli F, Grambow D, Muzik O, Mosca L, Rubenfire M, Schwaiger M. Early detection of abnormal coronary flow reserve in asymptomatic men at high risk for coronary artery disease using positron emission tomography. Circulation 1994;90:808–17. [PubMed: 8044952]
90. Laine H, Raitakari OT, Niinikoski H, et al. Early impairment of coronary flow reserve in young men with borderline hypertension. J Am Coll Cardiol 1998;32:147–53. [PubMed: 9669263]
91. Czernin J, Sun K, Brunken R, Bottcher M, Phelps M, Schelbert H. Effect of acute and long-term smoking on myocardial blood flow and flow reserve. Circulation 1995;91:2891–7. [PubMed: 7796497]
92. Cecchi F, Olivotto I, Gistri R, Lorenzoni R, Chiriatti G, Camici PG. Coronary microvascular dysfunction and prognosis in hypertrophic cardiomyopathy. N Engl J Med 2003;349:1027–35. [PubMed: 12968086]
93. Neglia D, Michelassi C, Trivieri MG, et al. Prognostic role of myocardial blood flow impairment in idiopathic left ventricular dysfunction. Circulation 2002;105:186–93. [PubMed: 11790699]
94. Zeiher AM, Krause T, Schachinger V, Minners J, Moser E. Impaired endothelium-dependent vasodilation of coronary resistance vessels is associated with exercise-induced myocardial ischemia. Circulation 1995;91:2345–52. [PubMed: 7729020]

95. Gould KL, Lipscomb K, Hamilton GW. Physiologic basis for assessing critical coronary stenosis. Instantaneous flow response and regional distribution during coronary hyperemia as measures of coronary flow reserve. Am J Cardiol 1974;33:87–94. [PubMed: 4808557]

96. Berman DS, Salel AF, DeNardo GL, Mason DT. Noninvasive detection of regional myocardial ischemia using rubidium-81 and the scintillation camera: Comparison with stress electrocardiography in patients with arteriographically documented coronary stenosis. Circulation 1975;52:619–26. [PubMed: 1157274]

97. Curtet C, Carlier T, Mirallie E, et al. Prospective comparison of two gamma probes for intraoperative detection of 18F-FDG: In vitro assessment and clinical evaluation in differentiated thyroid cancer patients with iodine-negative recurrence. Eur J Nucl Med Mol Imaging 2007;34:1556–62. [PubMed: 17522858]

98. Sampson UK, Dorbala S, Limaye A, Kwong R, Di Carli MF. Diagnostic accuracy of rubidium-82 myocardial perfusion imaging with hybrid positron emission tomography/computed tomography in the detection of coronary artery disease. J Am Coll Cardiol 2007;49:1052–8. [PubMed: 17349884]

99. Tamaki N, Yonekura Y, Senda M, et al. Value and limitation of stress thallium-201 single photon emission computed tomography: Comparison with nitrogen-13 ammonia positron tomography. J Nucl Med 1988;29:1181–8. [PubMed: 3260624]

100. Gould KL, Nakagawa Y, Nakagawa K, et al. Frequency and clinical implications of fluid dynamically significant diffuse coronary artery disease manifest as graded, longitudinal, base-to-apex myocardial perfusion abnormalities by noninvasive positron emission tomography. Circulation 2000;101:1931–9. [PubMed: 10779459]

101. Hernandez-Pampaloni M, Keng FY, Kudo T, Sayre JS, Schelbert HR. Abnormal longitudinal, base-to-apex myocardial perfusion gradient by quantitative blood flow measurements in patients with coronary risk factors. Circulation 2001;104:527–32. [PubMed: 11479248]

102. Berman DS, Kang X, Slomka PJ, et al. Underestimation of extent of ischemia by gated SPECT myocardial perfusion imaging in patients with left main coronary artery disease. J Nucl Cardiol 2007;14:521–8. [PubMed: 17679060]

103. Bateman TM, Heller GV, McGhie AI, et al. Diagnostic accuracy of rest/stress ECG-gated Rb-82 myocardial perfusion PET: Comparison with ECG-gated Tc-99m sestamibi SPECT. J Nucl Cardiol 2006;13:24–33. [PubMed: 16464714]

104. Dorbala S, Vangala D, Sampson U, Limaye A, Kwong R, Di Carli MF. Value of vasodilator left ventricular ejection fraction reserve in evaluating the magnitude of myocardium at risk and the extent of angiographic coronary artery disease: A 82Rb PET/CT study. J Nucl Med 2007;48:349–58. [PubMed: 17332611]

105. Parkash R, deKemp RA, Ruddy TD, et al. Potential utility of rubidium 82 PET quantification in patients with 3-vessel coronary artery disease. J Nucl Cardiol 2004;11:440–9. [PubMed: 15295413]

106. Kuhle WG, Porenta G, Huang SC, et al. Quantification of regional myocardial blood flow using 13 N-ammonia and reoriented dynamic positron emission tomographic imaging. Circulation 1992;86:1004–17. [PubMed: 1516170]

107. Sitek A, Gullberg GT, Huesman RH. Correction for ambiguous solutions in factor analysis using a penalized least squares objective. IEEE Trans Med Imaging 2002;21:216–25. [PubMed: 11989846]

108. El Fakhri G, Sitek A, Guerin B, Kijewski MF, Di Carli MF, Moore SC. Quantitative dynamic cardiac 82Rb PET using generalized factor and compartment analyses. J Nucl Med 2005;46:1264–71. [PubMed: 16085581]

109. Sharir T, Germano G, Kang X, et al. Prediction of myocardial infarction versus cardiac death by gated myocardial perfusion SPECT: Risk stratification by the amount of stress-induced ischemia and the poststress ejection fraction. J Nucl Med 2001;42:831–7. [PubMed: 11390544]

110. Brown TL, Merrill J, Volokh L, Bengel FM. Determinants of the response of left ventricular ejection fraction to vasodilator stress in electrocardiographically gated (82)rubidium myocardial perfusion PET. Eur J Nucl Med Mol Imaging 2008;35:336–42. [PubMed: 17912523]

111. Marwick TH, Shan K, Patel S, Go RT, Lauer MS. Incremental value of rubidium-82 positron emission tomography for prognostic assessment of known or suspected coronary artery disease. Am J Cardiol 1997;80:865–70. [PubMed: 9381999]

112. Yoshinaga K, Chow BJ, Williams K, et al. What is the prognostic value of myocardial perfusion imaging using rubidium-82 positron emission tomography? J Am Coll Cardiol 2006;48:1029–39. [PubMed: 16949498]
113. Dorbala S, Hachamovitch R, Curillova Z, et al. Incremental prognostic value of gated Rb-82 positron emission tomography myocardial perfusion imaging over clinical variables and rest LVEF. JACC Cardiovasc Imaging 2009;2:846–54. [PubMed: 19608135]
114. Lertsburapa K, Ahlberg AW, Bateman TM, et al. Independent and incremental prognostic value of left ventricular ejection fraction determined by stress gated rubidium 82 PET imaging in patients with known or suspected coronary artery disease. J Nucl Cardiol 2008;15:745–53. [PubMed: 18984449]
115. Yoshida K, Gould KL. Quantitative relation of myocardial infarct size and myocardial viability by positron emission tomography to left ventricular ejection fraction and 3-year mortality with and without revascularization. J Am Coll Cardiol 1993;22:984–97. [PubMed: 8409073]
116. Gould KL, Ornish D, Scherwitz L, et al. Changes in myocardial perfusion abnormalities by positron emission tomography after long-term, intense risk factor modification. JAMA 1995;274:894–901. [PubMed: 7674504]
117. Herzog BA, Husmann L, Landmesser U, Kaufmann PA. Low-dose computed tomography coronary angiography and myocardial perfusion imaging: Cardiac hybrid imaging below 3mSv. Eur Heart J 2009;30:644. [PubMed: 19036746]
118. Herzog BA, Husmann L, Valenta I, et al. Long-term prognostic value of 13 N-ammonia myocardial perfusion positron emission tomography added value of coronary flow reserve. J Am Coll Cardiol 2009;54:150–6. [PubMed: 19573732]
119. Schenker MP, Dorbala S, Hong EC, et al. Interrelation of coronary calcification, myocardial ischemia, and outcomes in patients with intermediate likelihood of coronary artery disease: A combined positron emission tomography/computed tomography study. Circulation 2008;117:1693–700. [PubMed: 18362235]
120. Blankstein R, Dorbala S. Adding calcium scoring to myocardial perfusion imaging: Does it alter physicians' therapeutic decision making? J Nucl Cardiol 2010;17:168–71. [PubMed: 20039150]
121. Raff GL, Gallagher MJ, O'Neill WW, Goldstein JA. Diagnostic accuracy of noninvasive coronary angiography using 64-slice spiral computed tomography. J Am Coll Cardiol 2005;46:552–7. [PubMed: 16053973]
122. Javadi M, Mahesh M, McBride G, et al. Lowering radiation dose for integrated assessment of coronary morphology and physiology: First experience with step-and-shoot CT angiography in a rubidium 82 PET-CT protocol. J Nucl Cardiol 2008;15:783–90. [PubMed: 18984453]
123. Pazhenkottil AP, Herzog BA, Husmann L, et al. Non-invasive assessment of coronary artery disease with CT coronary angiography and SPECT: A novel dose-saving fast-track algorithm. Eur J Nucl Med Mol Imaging 2010;37:522–7. [PubMed: 19789871]
124. Hachamovitch R, Johnson JR, Hlatky MA, et al. The study of myocardial perfusion and coronary anatomy imaging roles in CAD (SPARC): Design, rationale, and baseline patient characteristics of a prospective, multicenter observational registry comparing PET, SPECT, and CTA for resource utilization and clinical outcomes. J Nucl Cardiol 2009;16:935–48. [PubMed: 19760338]
125. Einstein AJ, Moser KW, Thompson RC, Cerqueira MD, Henzlova MJ. Radiation dose to patients from cardiac diagnostic imaging. Circulation 2007;116:1290–305. [PubMed: 17846343]
126. Stabin MG. Radiopharmaceuticals for nuclear cardiology: Radiation dosimetry, uncertainties, and risk. J Nucl Med 2008;49:1555–63. [PubMed: 18765586]
127. The 2007 recommendations of the international commission on radiological protection. ICRP publication 103. Ann ICRP 2007;37:1–332.
128. Dilsizian V, Narula J. Qualitative and quantitative scrutiny by regulatory process: Is the truth subjective or objective? JACC Cardiovasc Imaging 2009;2:1037–8. [PubMed: 19679295]
129. Nekolla SG, Reder S, Saraste A, et al. Evaluation of the novel myocardial perfusion positron-emission tomography tracer 18F-BMS-747158-02: comparison to 13 N-ammonia and validation with microspheres in a pig model. Circulation 2009;119:2333–42. [PubMed: 19380625]

130. Marwick TH, Nemec JJ, Stewart WJ, Salcedo EE. Diagnosis of coronary artery disease using exercise echocardiography and positron emission tomography: Comparison and analysis of discrepant results. J Am Soc Echocardiogr 1992;5:231–8. [PubMed: 1622613]

131. Grover-McKay M, Ratib O, Schwaiger M, et al. Detection of coronary artery disease with positron emission tomography and rubidium 82. Am Heart J 1992;123:646–52. [PubMed: 1539516]

132. Chow BJ, Al Shammeri OM, Beanlands RS, et al. Prognostic value of treadmill exercise and dobutamine stress positron emission tomography. Can J Cardiol 2009;25:e220–4. [PubMed: 19584976]

133. Castronovo, FP., Jr.; Schleipman, AR. Patient and occupational dosimetry. In: Di Carli, MF.; Lipton, MJ., editors. Cardiac PET and PET/CT imaging. Springer; 2007.

134. Kim KP, Einstein AJ, de Gonzalez A Berrington. Coronary artery calcification screening: Estimated radiation dose and cancer risk. Arch Intern Med 2009;169:1188–94. [PubMed: 19597067]

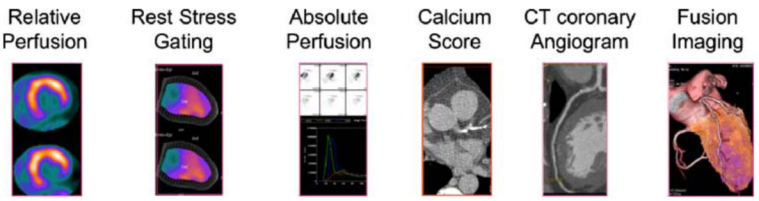

Figure 1.
Demonstrates the comprehensive imaging data (relative perfusion, rest and stress gated data, absolute perfusion, calcium score, CT coronary angiogram, and fused PET and CT coronary angiogram images) obtained by a list mode acquisition in a case of combined PET and CT coronary angiography.

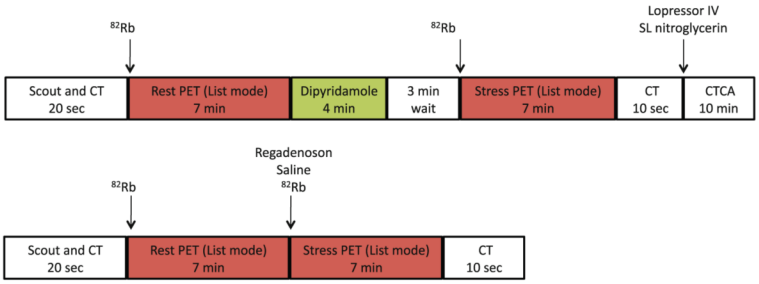

Figure 2.

A sample protocol for clinical cardiac PET/CT imaging with ^{82}Rb takes ~25 minutes. The use of Regadenoson stress makes the protocol ultrashort with completion of rest and stress imaging in ~17 minutes. *CT*, CT scan for attenuation correction; *CTCA*, CT coronary angiography; ^{82}*Rb*, ^{82}Rubidium.

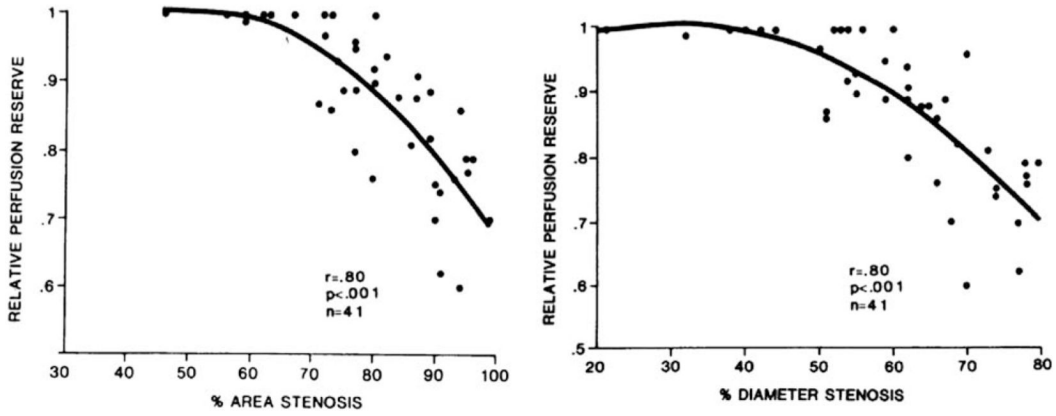

Figure 3.
Relative PET perfusion reserve as a tool to assess physiological significance of coronary stenoses. Reproduced with permission from Goldstein et al.[56]

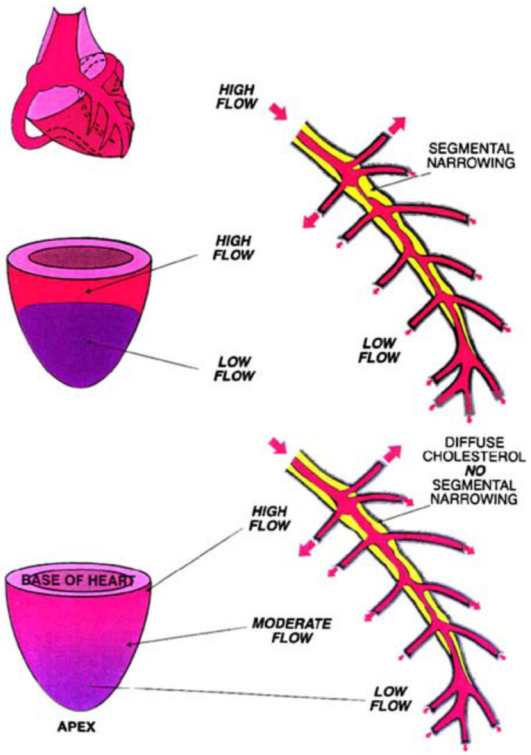

Figure 4.
Schematic demonstrating a discrete defect from a segmental coronary stenosis (*top*), in comparison to the gradual apex to base gradient that may be evident in cases of diffuse CAD. Reproduced with permission from Gould et al.[100]

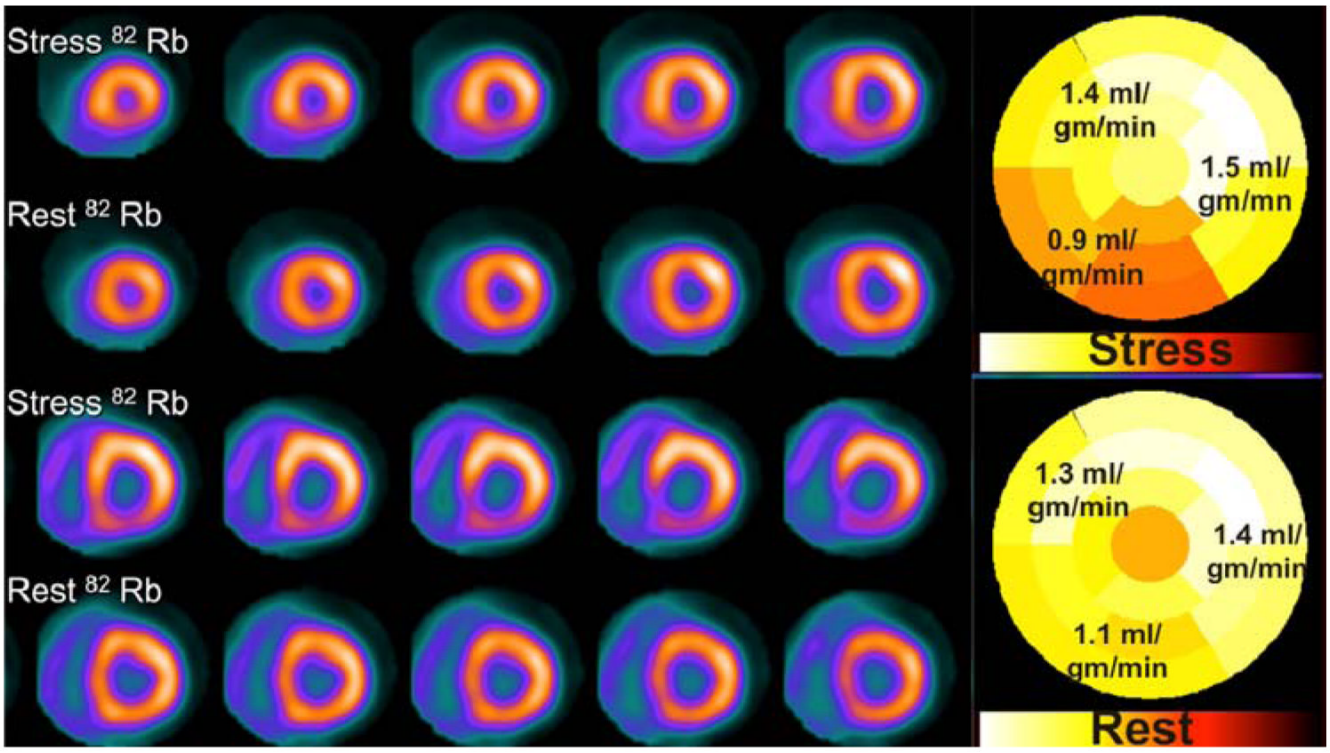

Figure 5.
Relative myocardial perfusion images demonstrate inferior and inferoseptal ischemia, while absolute myocardial perfusion is globally reduced, suggesting balanced ischemia.

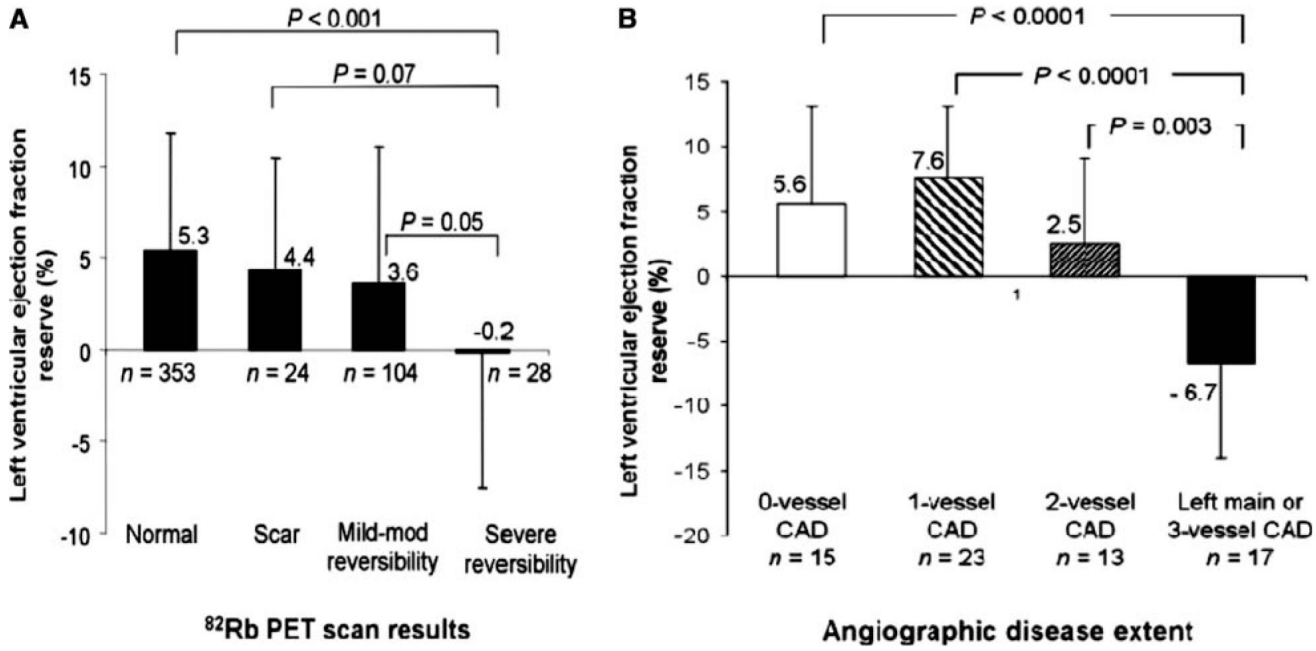

Figure 6.

Bar graphs demonstrating the relationship between LVEF reserve (peak stress minus rest LVEF) and the magnitude of stress-induced perfusion abnormalities (**A**) and the extent of angiographic CAD (>70% stenosis) (**B**). Reproduced with permission from Dorbala et al.[104]

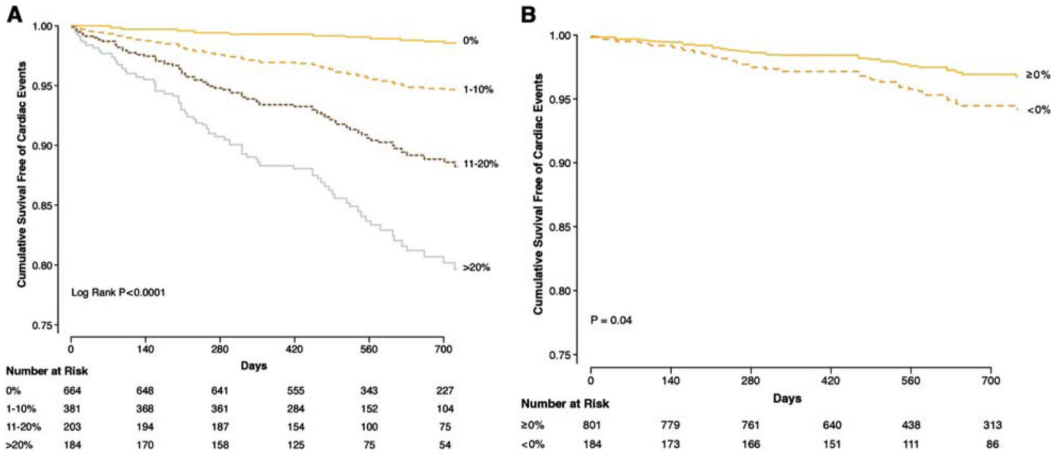

Figure 7.

(**A**) Risk adjusted survival curves demonstrating event free survival based on percent myocardium abnormal. Survival was excellent in patients with normal ^{82}Rb MPI (0% abnormal), and progressively worse survival was noted for patients with mild (1-10% abnormal), moderate (11-20% abnormal), or severely abnormal (≥20% abnormal) scans. (**B**) Risk adjusted survival curves demonstrating worse event free survival for patients with LVEF reserve <0%. Reproduced with permission from Dorbala et al.[113]

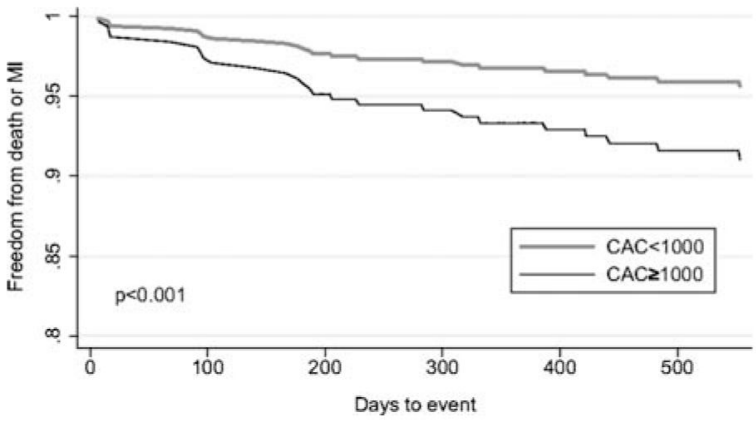

Figure 8.
Risk adjusted survival curves in patients with nonischemic relative PET scans demonstrating worse event free survival in patients with a calcium score (CAC) of ≥1000 compared to CAC <1000. Reproduced with permission from Schenker et al.[119]

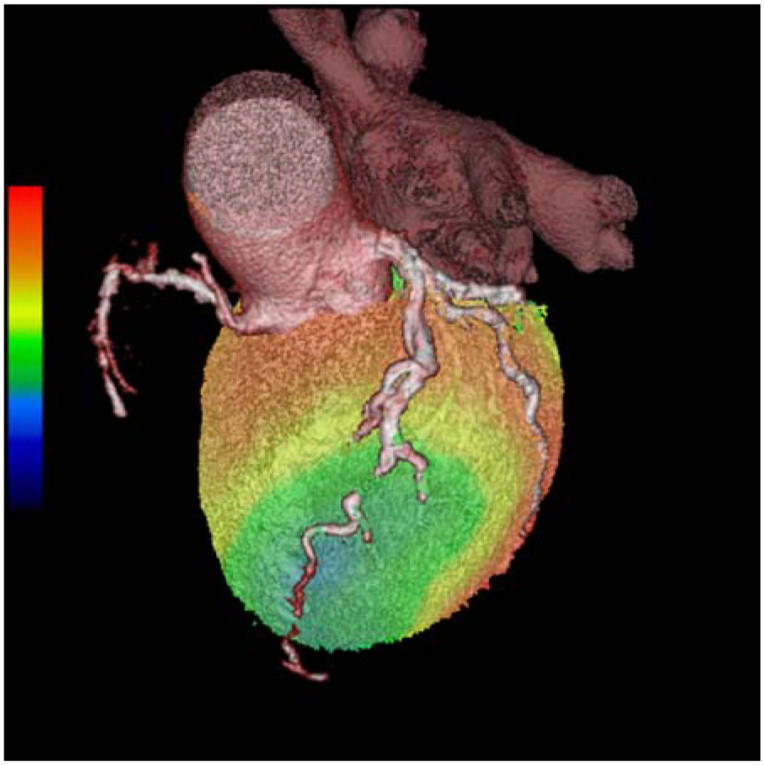

Figure 9.
A hybrid PET CTA examination in a patient with significant LAD ischemia. CT coronary angiogram image is overlaid on volume rendered stress ^{82}Rb perfusion image. CT coronary angiogram was performed to evaluate the patency/caliber of the distal LAD (beyond a known chronic total occlusion of the mid LAD) for consideration of coronary artery bypass surgery.

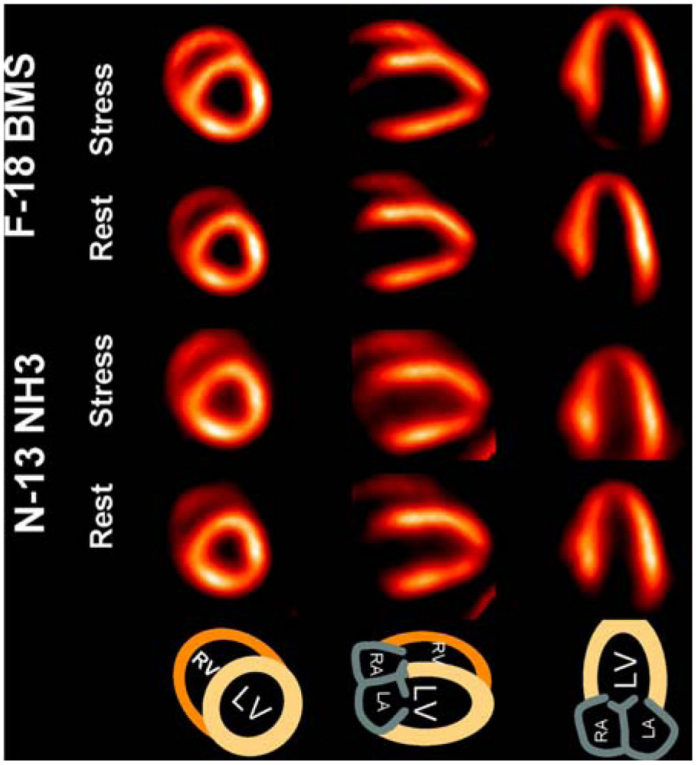

Figure 10.
Myocardial perfusion images using F-18 BMS showing comparable or better image quality compared to ^{13}N ammonia images. Reproduced with permission from Nekolla et al.[129]

Table 1

Summary of published literature regarding diagnostic accuracy of PET MPI

Author	Stress agent	Patients	Women	Prior CAD	PET Radiotracer	Sens	Spec	PPV	NPV	Accuracy
Sampson*[98]	Dipyridamole, adenosine, dobutamine	102	0.42	0	^{82}Rb	0.93	0.83	0.80	0.94	0.87
Bateman[103]	Dipyridamole	112	0.46	0.25	^{82}Rb	0.87	0.93	0.95	0.81	0.89
Marwick[130]	Dipyridamole + Hand grip	74	0.19	0.49	^{82}Rb	0.90	1	1	0.36	0.91
Grover-McKay[131]	Dipyridamole + Hand grip	31	0.01	0.13	^{82}Rb	1	0.73	0.80	1	0.87
Stewart[57]	Dipyridamole	81	0.36	0.42	^{82}Rb	0.83	0.86	0.94	0.64	0.84
Go[127]	Dipyridamole	202	NR	0.47	^{82}Rb	0.93	78	0.93	0.80	0.90
Demer[34]	Dipyridamole	193	0.26	0.34	^{82}Rb/$^{13}NH_3$	83	0.95	0.98	0.60	0.85
Tamaki[99]	Supine Bike	51	NR	0.75	$^{13}NH_3$	0.98	1	1	0.75	0.98
Gould[33]	Dipyridamole + Hand grip	31	NR	NR	^{82}Rb/$^{13}NH_3$	0.95	1	1	0.90	0.97
Weighted summary		877	0.29	0.35		0.90	0.89	0.94	0.73	0.90

Sens, Sensitivity; *Spec*, specificity; *PPV*, positive predictive value; *NPV*, negative predictive value.

*Study using PET/CT (where CT is used for attenuation correction only). Adapted with permission from Di Carli MF et al.[6]

Table 2

Percent abnormal myocardium in standard method vs. absolute perfusion reserve

Group	Standard method	Absolute method		
	Stress	Stress	Stress/rest absolute perfusion ratio	Stress-rest absolute perfusion reserve
3-vessel disease (% abnormal LV)	44% ± 18%	41% ± 29%	55% ± 25%	69% ± 24%†
1-vessel disease (% abnormal LV)	18% ± 17%	4% ± 7%*	9% ± 13%	10% ± 12%

*P = .01

†P = .008 compared with corresponding defect size by standard method. Table reproduced with permission from Parkash et al.[105]

Table 3

Summary of published literature regarding prognostic value of PET MPI

First author	Year	Stress agent	Tracer	Patients N	Events N	Event type	Prior CAD %	Percent normal scans (%)	Event/ yr in normal MPI (%)	Event/yr in abnormal MPI
Marwick[111]	1997	Dipyridamole	^{82}Rb	685	81	Cardiac death	Prior MI 48%, Prior Revas 37%	24	0.9	Mild 2.6%, moderate 5.1%, severe 5.1%
Yoshinaga[112]	2006	Dipyridamole	^{82}Rb	367	17	Cardiac death or MI	40.3%	70.5	0.4	2.3%, mild, 7.0% moderate-severe
Lertsburapa[114]	2009	Dipyridamole	^{82}Rb	1,441	132	All cause mortality	53.6%	64.8	2.4	4.1% mild, 6.9% moderate-severe
Dorbala[113]	2009	Dipyridamole Adenosine	^{82}Rb	1,432	140	Cardiac death or MI	30.6%	54	0.7	5.5% mild, 5% moderate, 11% severe
Herzog[118]	2009	Adenosine	^{13}N ammonia	256	29	Cardiac death	66%	45	0.5	3.1%
Chow[132]	2009	Exercise and dobutamine	^{82}Rb	124	16	Cardiac death, MI revasculari-zation	MI 40%, PCI 29%, CABG 15%	37	1.7	13%

^{82}*Rb*, ^{82}Rubidium; *MI*, non-fatal myocardial infarction

Table 4

Estimated effective radiation dose of common PET perfusion imaging studies

Test	Radiation dose (mSv)
^{82}Rb (rest + stress)[125]	12.6–13.5
^{13}N-ammonia (rest + stress)[125]	2.0–2.3
^{15}O-water (rest + stress)[125]	1.6–2.3
Scout/localizing CT[133]	0.04
CT attenuation correction[133]	0.35
Ca Scoring (Prospective gating)[134]	1.5–3